

Two-qubit gates using adiabatic passage of the Stark-tuned Förster resonances in Rydberg atoms

I. I. Beterov,^{1,2,3,*} M. Saffman,⁴ E. A. Yakshina,^{1,2} D. B. Tretyakov,^{1,2}
V. M. Entin,^{1,2} S. Bergamini,⁵ E. A. Kuznetsova,^{1,6} and I. I. Ryabtsev^{1,2}

¹*Rzhanov Institute of Semiconductor Physics SB RAS, 630090 Novosibirsk, Russia*

²*Novosibirsk State University, Interdisciplinary Quantum Center, 630090 Novosibirsk, Russia*

³*Novosibirsk State Technical University, 630073 Novosibirsk, Russia*

⁴*Department of Physics, University of Wisconsin-Madison, Madison, Wisconsin, 53706, USA*

⁵*The Open University, Walton Hall, MK7 6AA, Milton Keynes, UK*

⁶*Institute of Applied Physics RAS, 603950, Nizhny Novgorod, Russia*

We propose schemes of controlled-Z and controlled-NOT gates with ultracold neutral atoms based on deterministic phase accumulation during double adiabatic passage of the Stark-tuned Förster resonance of Rydberg states. Nonlinear time dependence of the energy detuning from the Förster resonance is used to achieve a high fidelity of population transfer between Rydberg states. Fidelity of two-qubit gates has been studied with an example of the $90S + 96S \rightarrow 90P + 95P$ Stark-tuned Förster resonance in Cs Rydberg atoms. We have found that off-resonant dipole-dipole interaction for different fine-structure levels results in additional phase shifts which can be partly compensated by an appropriately shaped electric-field pulse used for Stark tuning of Rydberg energy levels.

PACS numbers: 32.80.Ee, 03.67.Lx, 34.10.+x, 32.80.Rm

I. INTRODUCTION

Two-qubit quantum gates are the key element of a quantum computer. In general, any quantum algorithm can be implemented using a two-qubit controlled-NOT (CNOT) gate and single-qubit rotations [1]. Another example is a controlled-Z (CZ) gate which can be used for universal quantum computation as well as CNOT gate. Experimental implementation of high-fidelity two-qubit gates is a challenging task. A two-qubit gate error below 10^{-3} has been demonstrated recently for single-ion qubits [2, 3]. Scaling trapped ion qubits to very large quantum registers remains, however, an unsolved challenge. From this point of view, ultracold neutral atoms can be more promising candidates for implementation of a scalable quantum computer [4–8]. Arrays of optical dipole traps can be used as quantum registers of arbitrary dimensions [9], and the interaction of the atom qubits to perform two-qubit gates can be controlled by their temporary excitation to Rydberg states, which have large dipole moments and experience strong long-range interactions [4, 5, 10, 11]. For example, the effect of Rydberg excitation blockade [11] has been successfully applied in the experiment to implement a CNOT gate for ultracold neutral atoms with the fidelity above 0.73 [12]. At the same time, high-fidelity two-qubit gates with Rydberg atoms have not been demonstrated yet.

Another approach besides Rydberg blockade to building a two-qubit gate is based on controlled phase shifts of collective states of two qubits due to interaction between Rydberg atoms [4, 10]. The interaction strength should be adjusted to provide a certain phase shift (for exam-

ple π), during the interaction time. This can be easily done with Stark-tuned Förster resonances that provide fast and flexible control by manipulating the energies of Rydberg levels with an electric field [13–22]. The Rydberg levels are adjusted in such a way that one Rydberg level lies midway between two other Rydberg states of the opposite parity. Then a resonant energy transfer between Rydberg atoms initially excited to the middle state becomes possible via resonant dipole-dipole interaction. Stark-tuned Förster resonances for two Rydberg atoms were first reported in Ref. [23]. The rf-assisted Stark-tuned Förster resonances have been demonstrated in Refs. [24–27].

If two Rydberg atoms are frozen in space, dipole-dipole interaction at a Förster resonance induces the Rabi-like coherent population oscillations between collective states of these atoms [28]. Such oscillations have been demonstrated recently for two Rb Rydberg atoms in two optical dipole traps [29, 30]. The frequency of these collective oscillations is sensitive to variations of the interaction energy due to fluctuations of the spatial position of the atoms within the optical dipole traps. For example, a 10% variation of the distance between the trapped atoms results in a 25% variation of the interaction energy due to the $1/R^3$ dependence of the energy of dipole-dipole interaction on distance R between the atoms. This can substantially increase the phase gate error. In this paper we propose to overcome this difficulty by using a double adiabatic rapid passage across Stark-tuned Förster resonances with a deterministic phase accumulation. This technique is closely related to Stark-chirped rapid adiabatic passage, which is based on a laser-induced Stark shift [31, 32].

A scheme of CZ gate is shown in Fig. 1(a). Two optical dipole traps with one atom in each trap are located at a distance R between them. The two atoms are si-

* betarov@isp.nsc.ru

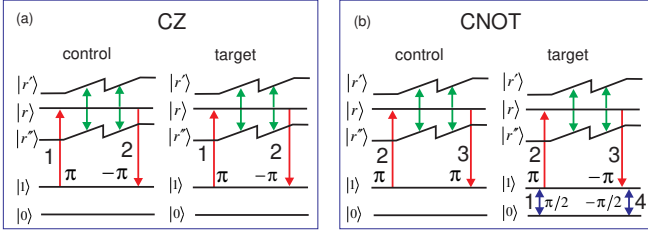


FIG. 1. (Color online) (a) Scheme of a CZ gate using double adiabatic rapid passage across Stark-tuned Förster resonance. Two atoms are excited to Rydberg states. An external electric field shifts the energy levels of the Rydberg atoms so that the Förster resonance is passed adiabatically two times. Then the atoms are de-excited to ground state. The phase shift is deterministically accumulated if both atoms are initially prepared in state $|1\rangle$; (b) Scheme of a CNOT gate. Two additional $\pi/2$ pulses rotate the target qubit around the y axis in the opposite directions.

multaneously excited to Rydberg state $|r\rangle$ by a π laser pulse labeled as 1. The distance between the traps must be sufficiently large to avoid the effect of Rydberg blockade [11]. A time-dependent external electric field shifts the collective energy levels so that the Förster resonance $|rr\rangle \rightarrow |r'r''\rangle$ is passed adiabatically two times. This results in a deterministic phase shift of state $|rr\rangle$. After the end of adiabatic passage the atoms are de-excited to ground state by a $-\pi$ laser pulse labeled as 2.

The phase shift due to Rydberg-Rydberg interaction is accumulated only in the case when both atoms are initially prepared in state $|1\rangle$ and then excited to Rydberg state $|r\rangle$. If one of the atoms (or both of them) is initially in the state $|0\rangle$, no phase shift occurs.

A scheme of CNOT gate is shown in Fig. 1(b). Two additional $\pi/2$ pulses, labeled as 1 and 4, rotate the target qubit around the y axis in the opposite directions. A $-\pi$ laser pulse (which is a π laser pulse with a π phase shift), acting on the control qubit in Fig. 1(a), is now replaced by the π pulse to avoid undesirable phase shift of the collective state. If the control qubit is initially prepared in state $|0\rangle$ and is not excited to Rydberg state, the pulse sequence acting on the target qubit returns it back to the initial state. The π phase shift due to the Rydberg-Rydberg interaction results in the inversion of the state of target qubit, if the control qubit is initially prepared in state $|1\rangle$.

The paper is organized as follows. In Sec. III we explain the effect of deterministic phase accumulation during double adiabatic rapid passage in a two-level quantum system. In Sec. IV we discuss the features of adiabatic rapid passage across Stark-tuned Förster resonance for two interacting Cs Rydberg atoms with nonlinear time dependence of the detuning from the resonance. Fine structure and finite lifetimes of the Rydberg states have been taken into account in our analysis.

II. PHASE ACCUMULATION DURING ADIABATIC RAPID PASSAGE

Adiabatic rapid passage is commonly used for laser excitation of molecular levels because of the independence of transition probability on the Rabi frequency [33]. A number of schemes for quantum logic using two-photon stimulated Raman adiabatic passage (STIRAP) [34] and Rydberg excitation has been developed [35, 36]. In our previous works [37, 38] we have found that double adiabatic rapid passage returns the system to the initial state, but with a deterministic phase shift. This shift is equal to π for two identical laser pulses and to zero if the second laser pulse has the opposite sign of Rabi frequency. This allowed us to develop schemes of quantum gates with mesoscopic atomic ensembles, using adiabatic passage and Rydberg blockade [37, 38]. Below we explain the effect of deterministic phase accumulation using a theory of adiabatic rapid passage [39]. The Hamiltonian for a two-level system with states $|1\rangle$ and $|2\rangle$, interacting with a chirped laser pulse (laser frequency and intensity change during the pulse), is written as

$$\hat{\mathbf{H}}(t) = \frac{\hbar}{2} \begin{pmatrix} -\delta(t) & \Omega_0(t) \\ \Omega_0(t) & \delta(t) \end{pmatrix}. \quad (1)$$

Here $\Omega_0(t)$ is time-dependent Rabi frequency and $\delta(t)$ is time-dependent detuning from the resonance. In the field interaction representation [39] the wavefunction is written as

$$\psi(t) = c_1(t) e^{i\omega t/2} |1\rangle + c_2(t) e^{-i\omega t/2} |2\rangle. \quad (2)$$

Here $c_1(t)$ and $c_2(t)$ are probability amplitudes and ω is laser frequency. We define the time-dependent basis states to be $|1(t)\rangle = e^{i\omega t} |1\rangle$ and $|2(t)\rangle = e^{-i\omega t} |2\rangle$. In this basis the wavefunction is rewritten as follows:

$$|\psi(t)\rangle = c_1(t) |1(t)\rangle + c_2(t) |2(t)\rangle. \quad (3)$$

To diagonalize the Hamiltonian, we rotate the basis:

$$\begin{pmatrix} |I(t)\rangle \\ |II(t)\rangle \end{pmatrix} = \mathbf{T}(t) \begin{pmatrix} |1(t)\rangle \\ |2(t)\rangle \end{pmatrix}. \quad (4)$$

Here $|I(t)\rangle$ and $|II(t)\rangle$ are semiclassical dressed states [39] and $\mathbf{T}(t)$ is time-dependent unitary rotation matrix:

$$\mathbf{T}(t) = \begin{pmatrix} \cos \theta(t) & -\sin \theta(t) \\ \sin \theta(t) & \cos \theta(t) \end{pmatrix}. \quad (5)$$

where $\theta(t)$ is a time-dependent mixing angle. The semiclassical dressed states are the superpositions:

$$\begin{aligned} |I(t)\rangle &= \cos \theta(t) |1(t)\rangle - \sin \theta(t) |2(t)\rangle \\ |II(t)\rangle &= \sin \theta(t) |1(t)\rangle + \cos \theta(t) |2(t)\rangle \end{aligned} \quad (6)$$

To derive the equation for the probability amplitudes of dressed states $\tilde{\mathbf{c}}$, we substitute the definition $\tilde{\mathbf{c}} = \mathbf{T}\mathbf{c}$ into the Schrödinger equation for the probability amplitudes $i\hbar\dot{\mathbf{c}} = \hat{\mathbf{H}}\mathbf{c}$. This results in

$$i\hbar\dot{\tilde{\mathbf{c}}} = \mathbf{T}\hat{\mathbf{H}}\mathbf{T}^\dagger\tilde{\mathbf{c}} - i\hbar\mathbf{T}\dot{\mathbf{T}}^\dagger\tilde{\mathbf{c}}. \quad (7)$$

The matrix $\mathbf{T}\hat{\mathbf{H}}\mathbf{T}^\dagger$ is diagonal if the mixing angle $\theta(t)$ obeys the following conditions:

$$\begin{aligned} \tan[2\theta(t)] &= \Omega_0(t)/\delta(t) \\ \sin[\theta(t)] &= \sqrt{\frac{1}{2}\left(1 - \frac{\delta(t)}{\Omega(t)}\right)} \\ \cos[\theta(t)] &= \sqrt{\frac{1}{2}\left(1 + \frac{\delta(t)}{\Omega(t)}\right)} \end{aligned} \quad (8)$$

Here $\Omega(t) = \sqrt{\Omega_0^2(t) + \delta(t)^2}$. This leads to:

$$\begin{aligned} \hat{\mathbf{H}}_d &= \mathbf{T}\hat{\mathbf{H}}\mathbf{T}^\dagger = \frac{\hbar}{2} \begin{pmatrix} -\Omega(t) & 0 \\ 0 & \Omega(t) \end{pmatrix} \\ \mathbf{T}\dot{\mathbf{T}}^\dagger &= i\sigma_y\dot{\theta} \end{aligned} \quad (9)$$

In the adiabatic approximation, when $|\dot{\Omega}_0(t)|/\Omega^2(t) \ll 1$ and $|\dot{\delta}(t)|/\Omega^2(t) \ll 1$ we can neglect the term proportional to $\dot{\theta}$. Then Eq. (7) is rewritten as $i\hbar\dot{\tilde{\mathbf{c}}} = \hat{\mathbf{H}}_d\tilde{\mathbf{c}}$. Its solution is

$$\begin{aligned} \tilde{c}_1(t) &= \tilde{c}_1(0) \exp\left[-i\int_0^t \Omega(t) dt\right] \\ \tilde{c}_2(t) &= \tilde{c}_2(0) \exp\left[i\int_0^t \Omega(t) dt\right] \end{aligned} \quad (10)$$

Now we consider a double adiabatic sequence which starts at $t=0$. The time dependence of Rabi frequency $\Omega_0(t)$ and detuning $\delta(t)$ is illustrated in Fig. 2(a). The system is initially in state $|1(t)\rangle$. For initial positive detuning $\delta(0) > 0$ and $\Omega_0(0) = 0$ we find $\Omega(0) = \delta(0)$ and therefore $\theta(0) = 0$. From Eq. (6) the initial dressed state is $|I(t)\rangle$ and $\tilde{c}_1(0) = 1$. The time-dependent probability amplitudes are

$$\begin{aligned} c_1(t) &= \tilde{c}_1(t) \cos\theta(t) \\ c_2(t) &= -\tilde{c}_1(t) \sin\theta(t) \end{aligned} \quad (11)$$

After the end of the first adiabatic passage at time T the detuning is negative $\delta(T) < 0$ and $\Omega(T) = -\delta(T)$. Therefore the mixing angle $\theta(T) = \pi/2$, and the system ends in state $|2(t)\rangle$ with $c_2(T) = -\tilde{c}_1(T) = -\exp\left[-i\int_0^T \Omega(t) dt\right] = -\exp[-iS]$. Here S is a generalized pulse area.

We denote the mixing angle and the probability amplitudes for the second adiabatic passage as θ' , $c'_1(t)$, $c'_2(t)$,

$\tilde{c}'_1(t)$, $\tilde{c}'_2(t)$. At the beginning of the second adiabatic passage the detuning is positive $\delta(T) > 0$ and $\theta'(T) = 0$. At time $t = T$ the system is in state $|2(t)\rangle$. From Eq. (6) the dressed state is now $|II(t)\rangle$. The probability amplitude $c_2(t)$ of state $|2(t)\rangle$ is constant around $t = T$ due to the absence of interaction with the laser field. Therefore, the initial probability amplitude of dressed state $|II(t)\rangle$ is $\tilde{c}'_2(T) = c_2(T) = -\tilde{c}_1(T)$. During the second adiabatic passage the time-dependent probability amplitudes are expressed similarly to Eq. (11):

$$\begin{aligned} c'_1(t) &= \tilde{c}'_2(t) \sin\theta'(t) \\ c'_2(t) &= \tilde{c}'_2(t) \cos\theta'(t) \end{aligned} \quad (12)$$

From Eq. (10) the probability amplitude of dressed state $|II(t)\rangle$ is $\tilde{c}'_2(t) = \tilde{c}'_2(T) \exp\left[-i\int_T^t \Omega(t) dt\right]$. After the end of the second adiabatic passage the mixing angle is $\theta'(2T) = \pi/2$ and the system ends in state $|1(t)\rangle$ with probability amplitude

$$\begin{aligned} c'_1(2T) &= \tilde{c}'_2(2T) = \\ &= -\exp\left[i\int_T^{2T} \Omega(t) dt\right] \exp\left[-i\int_0^T \Omega(t) dt\right] \end{aligned} \quad (13)$$

For two identical laser pulses we find $c'_1(2T) = -1$.

This π phase shift can be compensated if the second laser pulse has the opposite sign of Rabi frequency $\Omega_0 \rightarrow -\Omega_0$ (or a π phase shift of the laser field), as shown in Fig. 2(b). To diagonalize the Hamiltonian for the second adiabatic passage, we modify Eq. (8):

$$\begin{aligned} \tan[2\theta(t)] &= -\Omega_0(t)/\delta(t) \\ \sin[\theta(t)] &= -\sqrt{\frac{1}{2}\left(1 - \frac{\delta(t)}{\Omega(t)}\right)} \\ \cos[\theta(t)] &= \sqrt{\frac{1}{2}\left(1 + \frac{\delta(t)}{\Omega(t)}\right)} \end{aligned} \quad (14)$$

In this case after the end of the second adiabatic passage $\theta'(2T) = -\pi/2$ and $c'_1(2T) = 1$.

To illustrate this model we have numerically calculated the time dynamics of probability amplitudes of a two-level atom interacting with two chirped laser pulses with time-dependent Rabi frequency $\Omega_{0j}(t) = \Omega_0 \exp\left[-(t-t_j)^2/2w^2\right]$ and detuning $\delta_j(t) = s_1(t-t_j)$; where $j=1,2$, as shown in Fig. 2(a). The peak Rabi frequency is $\Omega_0/2\pi = 20$ MHz, the chirp of detuning is $s_1/2\pi = -50$ MHz/ μs , and the pulse width is $w = 0.12$ μs . The centers of the pulses are located at the times $t_1 = 0.5$ μs and $t_2 = 1.5$ μs . The conditions of Fig. 2(b) are similar, but the second pulse has the opposite sign of Rabi frequency. Figures 2(c) and 2(d) show the numerically calculated time dependence of probability $P_1 = |c_1(t)|^2$ to find the system in initial

with $\Omega_0/2\pi = 2$ MHz, $w = 0.12 \mu s$, and $\delta_k(t) = s_1(t - t_k)$ with $s_1 = -10$ MHz/ μs . For the right-hand panel of Fig. 3 Rabi frequency is constant $\Omega_{0k}(t)/2\pi = 2.1$ MHz, and the detuning is described by Eq. (15) with $s_1/2\pi = -10$ MHz/ μs , and $s_2/2\pi = -2600$ MHz/ μs^5 . The centers of the pulses are located at times $t_1 = 0.45 \mu s$ and $t_2 = 1.35 \mu s$. The population error for the final state of the system is found to be below 3×10^{-5} in both cases. The phase shift is equal to π in both cases.

Stark-tuned Förster resonance required for the implementation of the proposed scheme must meet the following criteria: (i) the lifetimes of Rydberg states must be sufficiently long to avoid the decay of coherence during the gate operation due to spontaneous and blackbody radiation (BBR) induced transitions; (ii) initial Förster energy defect must be sufficiently large to allow for rapid turning off the interaction between atoms at the beginning and the end of the adiabatic passage; (iii) selected interaction channel must be well isolated from the other channels to avoid break-up or dephasing of the adiabatic population transfer.

In our previous work [41] we have studied the structure of the Förster resonances $|nS, n'S\rangle \rightarrow |nP, (n' - 1)P\rangle$ in Rb and Cs Rydberg atoms. The energy defect for Cs $|nS, (n + 6)S\rangle \rightarrow |nP, (n + 5)P\rangle$ Förster resonance in a zero electric field is shown in Fig. 4(a) for the range of principal quantum numbers $80 < n < 130$. We have selected the $|90S_{1/2}, 96S_{1/2}\rangle \rightarrow |90P_{1/2}, 95P_{1/2}\rangle$ Stark-tuned Förster resonance for the further numerical simulations. This resonance has the energy defect $\delta_0/2\pi = 75.6$ MHz in a zero electric field. In contrast to the resonances involving $|nP_{3/2}\rangle$ states, this resonance has no Stark splitting in the electric field.

The Stark diagram for Cs Rydberg states with $|m_j| = 1/2$ is shown in Fig. 4(b). The dc electric field is aligned along the z axis. The $90S$ state is selected as zero energy level. We have calculated the radial matrix elements using the quasiclassical approximation [42] and the method of quantum defects [43–45]. The Stark shift for nS and nP Rydberg states is close to quadratic and is approximated as

$$\delta(E) = -\frac{1}{2}\alpha E^2. \quad (16)$$

The polarizabilities α , listed in Table I, have been found from the numeric approximation of the Stark energy shift for the electric field $E < 50$ mV/cm. The exact Förster resonance $|90S_{1/2}, 96S_{1/2}\rangle \rightarrow |90P_{1/2}, 95P_{1/2}\rangle$ occurs in the electric field $E = 29.73$ mV/cm.

For the initial collective state $|90S_{1/2}, m_a = 1/2; 96S_{1/2}, m_b = 1/2\rangle$ there are eight Förster interaction channels $|\gamma_a m_a, \gamma_b m_b\rangle \rightarrow |\gamma_\alpha m_\alpha, \gamma_\beta m_\beta\rangle$ listed in Table II and shown in Fig. 4(c). We have checked that the influence of the Förster resonance $|90P_{1/2}, 95P_{1/2}\rangle \rightarrow |88D_{3/2}, 95D_{3/2}\rangle$ with the detuning 288.9 MHz in zero electric field is negligible.

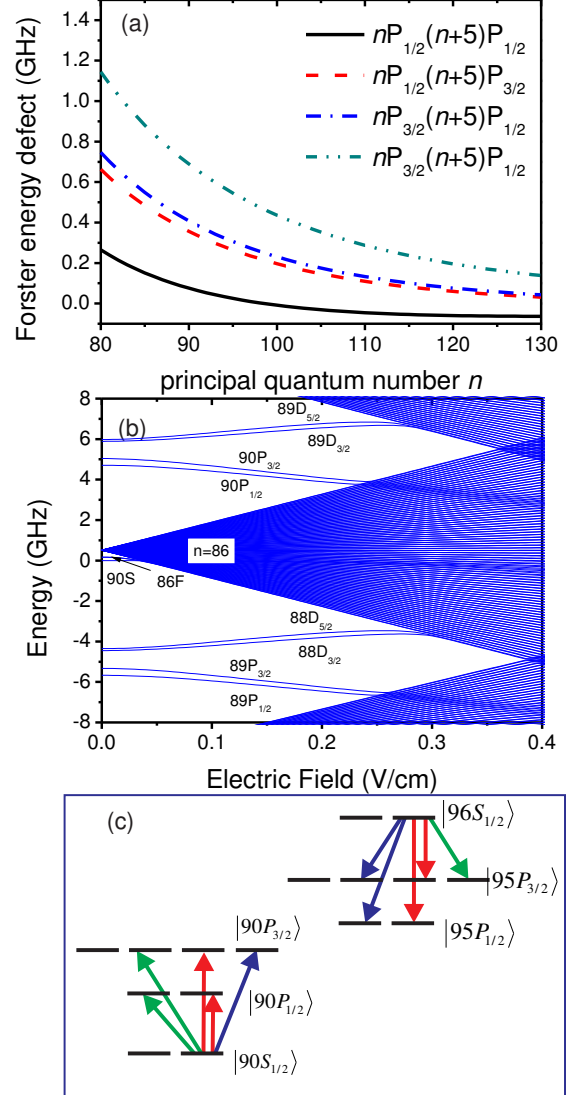


FIG. 4. (Color online) (a) Energy defect of the Förster resonance $|nS, (n + 6)S\rangle \rightarrow |nP, (n + 5)P\rangle$ in Cs Rydberg atoms; (b) Stark diagram for Cs Rydberg states with $|m_j| = 1/2$. The $90S$ state is selected as zero energy level; (c) Scheme of possible transitions for various channels of the $|90S, 96S\rangle \rightarrow |90P, 95P\rangle$ Förster resonance in Cs. The nS states with $m_j = 1/2$ are initially excited.

The operator of dipole interaction between atoms A and B with interatomic separation R along the z axis is

$$V_{dd} = \frac{e^2}{4\pi\epsilon_0 R^3} (\mathbf{a} \cdot \mathbf{b} - 3a_z b_z). \quad (17)$$

Here \mathbf{a} is a vectorial position of the electron in atom A and \mathbf{b} is a vectorial position of the electron in atom B [46]. For the states $|\gamma_a\rangle = |90S\rangle$, $|\gamma_b\rangle = |96S\rangle$, $|\gamma_\alpha\rangle = |90P\rangle$ and $|\gamma_\beta\rangle = |95P\rangle$ the matrix elements for the dipole-dipole interaction operator are written as [41]

TABLE I. Calculated polarizabilities of Cs Rydberg states

State	$ m_j $	α MHz (V/cm) ²
$ 90S_{1/2}\rangle$	1/2	3505
$ 96S_{1/2}\rangle$	1/2	5529
$ 90P_{1/2}\rangle$	1/2	72511
$ 90P_{3/2}\rangle$	1/2	103738
$ 90P_{3/2}\rangle$	3/2	87196
$ 95P_{1/2}\rangle$	1/2	107380
$ 95P_{3/2}\rangle$	1/2	153574
$ 95P_{3/2}\rangle$	3/2	129118

TABLE II. Förster resonance channels $|\gamma_a m_a, \gamma_b m_b\rangle \rightarrow |\gamma_\alpha m_\alpha, \gamma_\beta m_\beta\rangle$ and their angular factors. Here $m_a = m_b = 1/2$.

	$ \gamma_a\rangle$	$ \gamma_b\rangle$	$ \gamma_\alpha\rangle$	$ \gamma_\beta\rangle$	m_α	m_β	Q_k
1	$90S_{1/2}$	$96S_{1/2}$	$90P_{1/2}$	$95P_{1/2}$	1/2	1/2	$-2/3$
2	$90S_{1/2}$	$96S_{1/2}$	$90P_{1/2}$	$95P_{3/2}$	1/2	1/2	$-2\sqrt{2}/3$
3	$90S_{1/2}$	$96S_{1/2}$	$90P_{1/2}$	$95P_{3/2}$	-1/2	3/2	$-\sqrt{2}/3$
4	$90S_{1/2}$	$96S_{1/2}$	$90P_{3/2}$	$95P_{1/2}$	1/2	1/2	$-2\sqrt{2}/3$
5	$90S_{1/2}$	$96S_{1/2}$	$90P_{3/2}$	$95P_{1/2}$	3/2	-1/2	$-\sqrt{2}/3$
6	$90S_{1/2}$	$96S_{1/2}$	$90P_{3/2}$	$95P_{3/2}$	1/2	1/2	$-4/3$
7	$90S_{1/2}$	$96S_{1/2}$	$90P_{3/2}$	$95P_{3/2}$	-1/2	3/2	$-1/\sqrt{3}$
8	$90S_{1/2}$	$96S_{1/2}$	$90P_{3/2}$	$95P_{3/2}$	3/2	-1/2	$-1/\sqrt{3}$

$$M_{m_a, m_b}^{m_\alpha, m_\beta} = \frac{C_{3,k}}{R^3} Q_k \quad (18)$$

$$Q_k = -\sqrt{6} \sum_{q=-1}^1 C_{1q1-q}^{20} C_{j_a m_a 1q}^{j_\alpha m_\alpha} C_{j_b m_b 1-q}^{j_\beta m_\beta}.$$

Here Q_k is the angular factor (see Table II) which is only nonzero for $m_a + m_b = m_\alpha + m_\beta$, and the dipole-dipole interaction energy $C_{3,k}$ coefficient is expressed as

$$C_{3,k}(a, b, \alpha, \beta) = q^2 \frac{\langle \gamma_\alpha || r_a || \gamma_a \rangle \langle \gamma_\beta || r_b || \gamma_b \rangle}{\sqrt{(2j_\alpha + 1)(2j_\beta + 1)}}, \quad (19)$$

with $q^2 = e^2/4\pi\epsilon_0$, e is the electronic charge, ϵ_0 is the permittivity of free space, and $\langle \gamma_\alpha || r_a || \gamma_a \rangle$ is a reduced matrix element in the fine structure basis:

$$\langle \gamma_\alpha || r || \gamma_a \rangle = (-1)^{\frac{l_\alpha + l_a}{2} + j_a} \sqrt{\max(l_\alpha, l_a)} \times \quad (20)$$

$$\times \sqrt{2j_\alpha + 1} \sqrt{2j_a + 1} \begin{Bmatrix} l_\alpha & 1/2 & j_a \\ j_\alpha & 1 & l_a \end{Bmatrix} r.$$

Here r is the radial matrix element.

The time dependence of the electric field required to form the nonlinearly shaped detuning $\delta_k(t) = s_1(t - t_k) + s_2(t - t_k)^5$ of the $|90S_{1/2}, 96S_{1/2}\rangle \rightarrow$

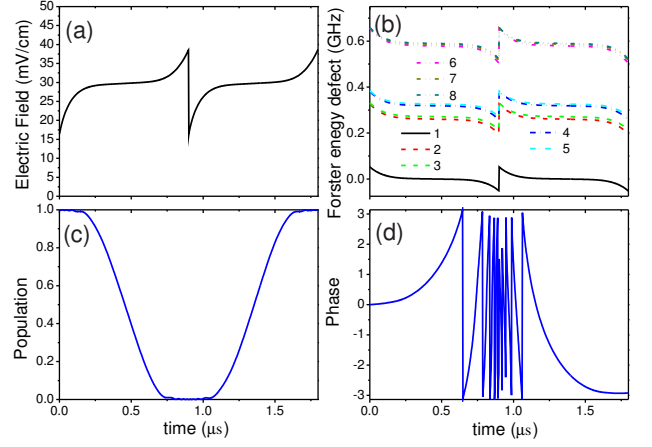


FIG. 5. (Color online) (a) Time dependence of the electric field for Stark tuning of the $|90S_{1/2}, 96S_{1/2}\rangle \rightarrow |90P_{1/2}, 95P_{1/2}\rangle$ Förster resonance; (b) Time dependence of the energy defects of the interaction channels listed in Table I for the $|90S, 96S\rangle \rightarrow |90P, 95P\rangle$ Förster resonance; (c) Time dependence of the population of the collective state $|90S_{1/2}, 96S_{1/2}\rangle$; (d) Time dependence of phase of the collective state $|90S_{1/2}, 95S_{1/2}\rangle$.

$|90P_{1/2}, 95P_{1/2}\rangle$ Förster resonance with $s_1/2\pi = -10$ MHz/ μs and $s_2/2\pi = -2600$ MHz/ μs^5 , $t_1 = 450$ ns and $t_2 = 1350$ ns is shown in Fig. 5(a). The time dependent Förster energy defects for all eight channels are shown in Fig. 5(b). The off-resonant excitation of various Förster channels, partial overlapping of the resonances, and the finite lifetimes of Rydberg states are the most important limiting factors for quantum gate performance.

The time dependence of the population [Fig. 5(c)] and phase [Fig. 5(d)] of the collective $|90S_{1/2}, 96S_{1/2}\rangle$ state for two interacting Rydberg atoms located at distance $R=25 \mu m$ along the z axis was calculated taking into account all eight interaction channels from Table I. The off-resonant interaction channels lead to the undesirable phase shift, which is clearly seen in Fig. 5(d). This shift can be partly compensated by adjusting the shape of the electric-field pulse, for example, by changing the time position of the second resonance to $t_2 = 1350.6$ ns.

With this correction we have calculated the time dependence of population and phase of the collective $|90S_{1/2}, 96S_{1/2}\rangle$ state for slightly different interatomic distances $R=24 \mu m$ (left-hand panel in Fig. 6), $R=25 \mu m$ (central panel in Fig. 6) and $R=26 \mu m$ [right-hand panel in Fig. 6(b)]. Our calculations have shown that this variation of the interatomic distance leads to small phase changes at the end of the adiabatic passage, thus evidencing that our method to perform two-qubit quantum gates is insensitive to the atom position uncertainty.

To estimate the fidelity of our schemes for two-qubit gates in realistic experimental conditions we have numerically calculated the truth table of a CNOT gate [Fig. 1]

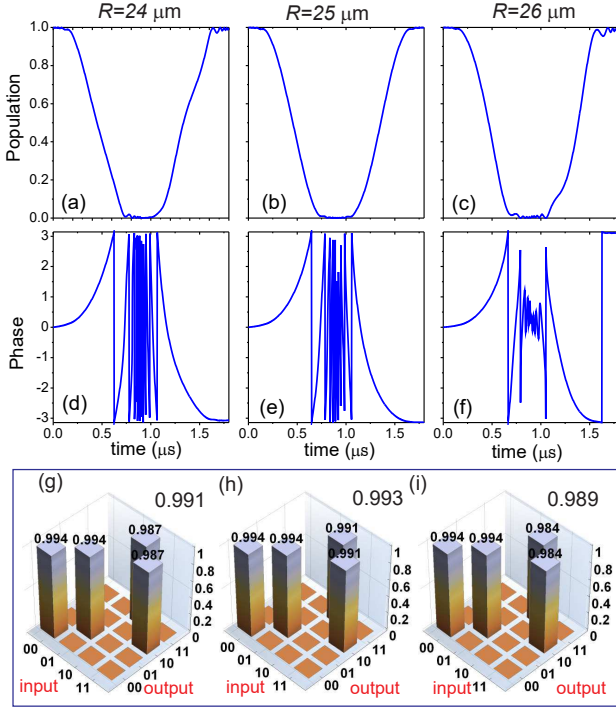


FIG. 6. (Color online) Double adiabatic passage of the Stark-tuned Förster resonance for different interatomic distances R with error correction. (a), (b), (c) Time dependences of population of the collective state $|90S_{1/2}, 96S_{1/2}\rangle$ calculated for $R=24, 25$ and $26 \mu\text{m}$, respectively; (d), (e), (f) Time dependences of phase of the collective state $|90S_{1/2}, 96S_{1/2}\rangle$ calculated for $d=24, 25$ and $26 \mu\text{m}$, respectively; (g), (h), (i) Calculated truth tables of a CNOT gate for $R=24, 25$ and $26 \mu\text{m}$, respectively. The overlap with the ideal truth table is shown above each plot.

using a master equation for the density matrix and taking into account finite lifetimes of the Rydberg levels. We neglected a repopulation of the ground state during decay of the Rydberg states because of the blackbody-radiation induced transfer to neighboring Rydberg states is the major decay channel for high Rydberg states [47]. The truth tables were calculated for the same interatomic distances as previously ($R=24, 25$ and $26 \mu\text{m}$). We have finally found that for $R=25 \mu\text{m}$ the error is less than 1%, and it only slightly increases when the distance between the atoms is varied. The main source of this error is revealed to be finite lifetimes of Rydberg atoms. In a 300 K environment the Rydberg states used have lifetimes [47] $\tau_{90S} = 270 \mu\text{s}$, $\tau_{96S} = 314 \mu\text{s}$, $\tau_{90P} = 361 \mu\text{s}$, $\tau_{95P} = 406 \mu\text{s}$.

We have studied the phase errors by calculation of the fidelity of the Bell states which are created by Hadamard gate applied to a control qubit, and a subsequent CNOT applied to a pair of qubits. The Bell states of a bipartite

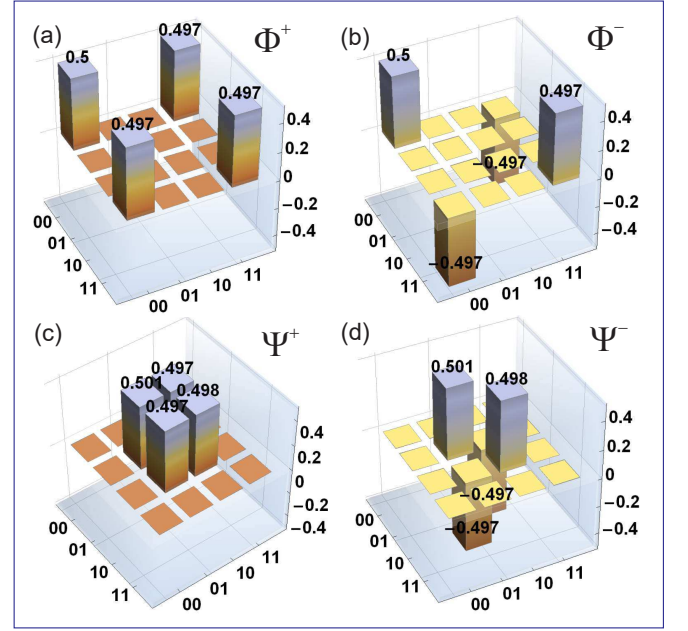


FIG. 7. (Color online) The reconstructed density matrices of the (a) Φ^+ , (b) Φ^- , (c) Ψ^+ and (d) Ψ^- Bell states.

quantum system are defined as following:

$$\begin{aligned}\Phi^+ &= \frac{1}{\sqrt{2}} (|00\rangle + |11\rangle) \\ \Phi^- &= \frac{1}{\sqrt{2}} (|00\rangle - |11\rangle) \\ \Psi^+ &= \frac{1}{\sqrt{2}} (|01\rangle + |10\rangle) \\ \Psi^- &= \frac{1}{\sqrt{2}} (|01\rangle - |10\rangle).\end{aligned}\quad (21)$$

The density matrices of the generated Bell states after using maximum-likelihood reconstruction are shown in Fig. (7) for interatomic distance $R = 25 \mu\text{m}$. The calculated Bell state fidelities taking into account Rydberg lifetimes were better than 0.99. For $R = 24 \mu\text{m}$ and $R = 26 \mu\text{m}$ the fidelities are reduced to 0.96 and 0.98, respectively. Variation of the delay of the second resonance by 100 ps also reduces the Bell fidelities to 0.97 at $R = 25 \mu\text{m}$.

Atomic qubits trapped in an optically defined array are subject to only small position variations. For example using trap parameters from [12, 48] and assuming an atom temperature of $T = 10 \mu\text{K}$ gives an in-plane position standard deviation of $\delta x \sim 0.1 \mu\text{m}$ and an out of plane variation of $\delta z \sim 1.5 \mu\text{m}$. This implies a variation around the $25 \mu\text{m}$ nominal separation of $\pm 0.15 \mu\text{m}$. Comparing with Fig. 6 we anticipate less than 0.001 variation in gate fidelity for these conditions. Our calculations therefore show that the proposed gate protocol is insensitive to realistic experimental variations in the atom position.

IV. SUMMARY

We investigated the adiabatic passage across a Förster resonance which can be considered as an alternative to the Rydberg blockade for implementation of two-qubit quantum gates with Rydberg atoms.

The gate fidelity has been found to be limited mainly by finite lifetimes of Rydberg states and dephasing due to off-resonant excitation of various Förster interaction channels. The decay of Rydberg population during the gate gives the radiative decay error of approximately 10^{-2} which is close to the calculated gate error in Fig. 6(h) and Fig 7. Reducing this error requires shorter gate times and larger separation from the neighboring Förster resonances which can be observed only for the lower states with shorter lifetimes [see Fig. 4(a)]. Although quantum gates based on Rydberg blockade in theory could provide the errors below 10^{-4} [49], such fidelity has not yet been demonstrated experimentally.

In contrast to the Rydberg-blockade gates, our approach does not require strong interaction between Rydberg atoms and can be potentially advantageous for implementing gates at large interatomic spacings. Although a 10^{-4} gate error is widely considered to be necessary for scalable quantum computation with a realistic overhead in terms of the number of physical qubits the availability of long range gates with lower fidelity can be a useful feature of a large scale architecture. In order to move

quantum information between qubits with large physical separation one can execute a string of swap gates using high fidelity local operations. The alternative is to use a lower fidelity gate that operates at long range to create Bell pairs with moderate fidelity, followed by entanglement purification with local operations [50], and teleportation [51]. The gate protocol analyzed here provides CNOT truth table fidelity of > 0.99 and creates maximally entangled Bell pairs with fidelity > 0.99 . With a qubit spacing of $\sim 4 \mu\text{m}$ in a 2D array [12] the $R = 25 \mu\text{m}$ range gate we analyze here would enable entanglement of arbitrary pairs in a block of 25 qubits suitable for encoding medium sized logical qubits.

The Förster resonances in time-varying electric field have been recently studied experimentally [27]. It has been shown that even for moderate interaction strengths it is possible to observe them on a short timescale of 100 ns.

This work was supported by the Russian Science Foundation Grant No. 16-12-00028 in the part of numeric simulation of the two-qubit gates and Bell states, by RFBR Grants No. 14-02-00680 and 16-02-00383, by Novosibirsk State University and Russian Academy of Sciences. MS was supported by NSF award 1521374, the AFOSR MURI on Quantum Memories and Light-Matter Interfaces, and the ARL-CDQI through cooperative agreement W911NF-15-2-0061. S.B. was supported by EP-SRC grant no EP/K022938/1.

-
- [1] M. A. Nielsen and I. L. Chuang, *Quantum Computation and Quantum Information* (Cambridge University Press, 2011).
 - [2] C. Ballance, T. P. Harty, N. M. Linke, M. A. Sepiol, and L. D. M., arXiv:1512.04600 (2015).
 - [3] J. P. Gaebler, T. R. Tan, Y. Lin, Y. Wan, R. Bowler, R. A. C. Keith, S. Glancy, K. Coakley, E. Knill, D. Leibfried, and D. J. Wineland, arXiv:1604.00032 (2016).
 - [4] I. I. Ryabtsev, D. B. Tretyakov, and I. I. Beterov, *Journal of Physics B: Atomic and Molecular Physics* **38**, S421 (2005).
 - [5] M. Saffman, T. G. Walker, and K. Mølmer, *Rev. Mod. Phys.* **82**, 2313 (2010).
 - [6] D. Comparat and P. Pillet, *J. Opt. Soc. Am. B* **27**, A208 (2010).
 - [7] I. Ryabtsev, I. Beterov, D. Tretyakov, V. Entin, and E. Yakshina, *Physics-Uspekhi* **59**, 196 (2016).
 - [8] M. Saffman, arxiv:1605.05207 (2016).
 - [9] T. Xia, M. Lichtman, K. Maller, A. W. Carr, M. J. Piotrowicz, L. Isenhower, and M. Saffman, *Phys. Rev. Lett.* **114**, 100503 (2015).
 - [10] D. Jaksch, J. I. Cirac, P. Zoller, S. L. Rolston, R. Côté, and M. D. Lukin, *Phys. Rev. Lett.* **85**, 2208 (2000).
 - [11] M. D. Lukin, M. Fleischhauer, R. Côté, L. M. Duan, D. Jaksch, J. I. Cirac, and P. Zoller, *Phys. Rev. Lett.* **87**, 037901 (2001).
 - [12] K. M. Maller, M. T. Lichtman, T. Xia, Y. Sun, M. J. Piotrowicz, A. W. Carr, L. Isenhower, and M. Saffman, *Phys. Rev. A* **92**, 022336 (2015).
 - [13] K. A. Safinya, J. F. Delpech, F. Gounand, W. Sandner, and T. F. Gallagher, *Phys. Rev. Lett.* **47**, 405 (1981).
 - [14] W. R. Anderson, J. R. Veale, and T. F. Gallagher, *Phys. Rev. Lett.* **80**, 249 (1998).
 - [15] I. Mourachko, D. Comparat, F. de Tomasi, A. Fioretti, P. Nosbaum, V. M. Akulin, and P. Pillet, *Phys. Rev. Lett.* **80**, 253 (1998).
 - [16] S. Westermann, T. Amthor, A. L. de Oliveira, J. Deiglmayr, M. Reetz-Lamour, and M. Weidemüller, *European Physical Journal D* **40**, 37 (2006).
 - [17] J. B. Balewski, A. T. Krupp, B. Butscher, R. Löw, and T. Pfau, *Phys. Rev. Lett.* **108**, 113001 (2012).
 - [18] B. G. Richards and R. R. Jones, *Phys. Rev. A* **93**, 042505 (2016).
 - [19] J. M. Kondo, D. Booth, L. F. Gonçalves, J. P. Shaffer, and L. G. Marcassa, *Phys. Rev. A* **93**, 012703 (2016).
 - [20] B. Pelle, R. Faoro, J. Billy, E. Arimondo, P. Pillet, and P. Cheinet, *Phys. Rev. A* **93**, 023417 (2016).
 - [21] A. Paris-Mandoki, H. Gorniaczyk, C. Tresp, I. Mirgorodskiy, and S. Hofferberth, arxiv:1605.00259 (2016).
 - [22] A. Browaeys, D. Barredo, and T. Lahaye, arXiv:1603.04603 (2016).
 - [23] I. I. Ryabtsev, D. B. Tretyakov, I. I. Beterov, and V. M. Entin, *Phys. Rev. Lett.* **104**, 073003 (2010).
 - [24] C. S. E. van Ditzhuijzen, A. Tauschinsky, and H. B. van Linden van den Heuvell, *Phys. Rev. A* **78**, 063409 (2008).
 - [25] C. S. E. van Ditzhuijzen, A. Tauschinsky,

- and H. B. van Linden van den Heuvell, Phys. Rev. A **80**, 063407 (2009).
- [26] D. B. Tretyakov, V. M. Entin, E. A. Yakshina, I. I. Beterov, C. Andreeva, and I. I. Ryabtsev, Phys. Rev. A **90**, 041403 (2014).
- [27] E. A. Yakshina, D. B. Tretyakov, I. I. Beterov, V. M. Entin, C. Andreeva, A. Cinins, A. Markovski, Z. Iftikhar, A. Ekers, and I. I. Ryabtsev, arXiv:1606.06016 (2016).
- [28] I. I. Ryabtsev, D. B. Tretyakov, I. I. Beterov, V. M. Entin, and E. A. Yakshina, Phys. Rev. A **82**, 053409 (2010).
- [29] S. Ravets, H. Labuhn, D. Barredo, L. Beguin, T. Lahaye, and A. Browaeys, Nature Physics **10**, 914 (2014).
- [30] S. Ravets, H. Labuhn, D. Barredo, T. Lahaye, and A. Browaeys, Phys. Rev. A **92**, 020701 (2015).
- [31] B. W. Shore, *Manipulating Quantum Structures Using Laser Pulses* (Cambridge University Press, 2011).
- [32] L. P. Yatsenko, N. V. Vitanov, B. W. Shore, T. Rickes, and K. Bergmann, Optics Communications **204**, 413 (2002).
- [33] V. S. Malinovsky and J. L. Krause, European Physical Journal D **14**, 147 (2001).
- [34] K. Bergmann, H. Theuer, and B. Shore, Review of Modern Physics **70**, 1003 (1998).
- [35] D. Møller, L. B. Madsen, and K. Mølmer, Phys. Rev. Lett. **100**, 170504 (2008).
- [36] D. D. B. Rao and K. Mølmer, Phys. Rev. A **89**, 030301 (2014).
- [37] I. I. Beterov, M. Saffman, E. A. Yakshina, V. P. Zhukov, D. B. Tretyakov, V. M. Entin, I. I. Ryabtsev, C. W. Mansell, C. McCormick, S. Bergamini, and M. P. Fedoruk, Phys. Rev. A **88**, 010303(R) (2013).
- [38] I. I. Beterov, M. Saffman, E. A. Yakshina, V. P. Zhukov, D. B. Tretyakov, V. M. Entin, I. I. Ryabtsev, C. W. Mansell, C. McCormick, S. Bergamini, and M. P. Fedoruk, Laser Physics **24**, 074013 (2014).
- [39] P. Berman and V. Malinovsky, eds., *Principles of Laser Spectroscopy and Quantum Optics* (Princeton University Press, 2011).
- [40] M. G. Bason, M. Viteau, N. Malossi, P. Huillery, E. Arimondo, D. Ciampini, R. Fazio, V. Giovannetti, R. Manna, and O. Morsch, Nature Physics **8**, 147 (2012).
- [41] I. I. Beterov and M. Saffman, Phys. Rev. A **92**, 042710 (2015).
- [42] L. G. Dyachkov and P. M. Pankratov, Journal of Physics B: Atomic and Molecular Physics **27**, 461 (1994).
- [43] C. J. Lorenzen and K. Niemax, Z. Phys. A - Atoms and Nuclei **315**, 127 (1984).
- [44] K.-H. Weber and C. J. Sansonetti, Phys. Rev. A **35**, 4650 (1987).
- [45] J. Deiglmayr, H. Herburger, H. Saßmannshausen, P. Jansen, H. Schmutz, and F. Merkt, Phys. Rev. A **93**, 013424 (2016).
- [46] T. G. Walker and M. Saffman, Phys. Rev. A **77**, 032723 (2008).
- [47] I. I. Beterov, I. I. Ryabtsev, D. B. Tretyakov, and V. M. Entin, Phys. Rev. A **79**, 052504 (2009).
- [48] M. J. Piotrowicz, M. Lichtman, K. Maller, G. Li, S. Zhang, L. Isenhower, and M. Saffman, Phys. Rev. A **88**, 013420 (2013).
- [49] L. Theis, F. Motzoi, F. K. Wilhelm, and M. Saffman, arXiv:1605.08891 (2016).
- [50] C. H. Bennett, G. Brassard, S. Popescu, B. Schumacher, J. A. Smolin, and W. K. Wootters, Phys. Rev. Lett. **76**, 722 (1996).
- [51] D. Gottesman and I. L. Chuang, Nature **402**, 390 (1999).